

## Sun–Earth connection: Boundary layer waves and auroras

G S LAKHINA<sup>1</sup>, B T TSURUTANI<sup>2</sup>, J K ARBALLO<sup>2</sup> and C GALVAN<sup>2</sup>

<sup>1</sup>Indian Institute of Geomagnetism, Colaba, Mumbai 400 005, India

<sup>2</sup>Jet Propulsion Laboratory, California Institute of Technology, 4800 Oak Grove Drive, Pasadena, California 91109, USA

**Abstract.** Boundary layers are the sites where energy and momentum are exchanged between two distinct plasmas. Boundary layers occurring in space plasmas can support a wide spectrum of plasma waves spanning a frequency range of a few mHz to 100 kHz and beyond. The main characteristics of the broadband plasma waves (with frequencies  $> 1$  Hz) observed in the magnetopause, polar cap, and plasma sheet boundary layers are described. The rapid pitch angle scattering of energetic particles via cyclotron resonant interactions with the waves can provide sufficient precipitated energy flux to the ionosphere to create the diffused auroral oval. The broadband plasma waves may also play an important role in the processes of local heating/acceleration of the boundary layer plasma.

**Keywords.** Wave-particle interactions; boundary layer waves; aurora.

**PACS Nos** 94.30.Di; 94.30.Tz; 94.10.Rk; 52.35.-g

### 1. Introduction

The boundary layers in space and astrophysical plasmas are generally formed when plasmas with different characteristics interact with each other. For the case of the Earth, the magnetopause boundary is formed by the interaction of the shocked solar wind plasma in the magnetosheath with the hot plasma in the magnetosphere. The magnetosheath is a region of shocked solar wind plasma downstream of the bow-shock that is formed ahead of the magnetopause to deflect the oncoming super-Alfvénic and supersonic solar wind plasma smoothly around the Earth, as the geomagnetic field forms an obstacle in its flow. At the bow shock, the solar wind gets heated and compressed. Several plasma measurements have identified the existence of a boundary layer, inside of and adjacent to the magnetopause, consisting of plasma with temperature and flow properties intermediate between the magnetosheath and the magnetosphere proper [1–4]. This boundary layer is referred to as magnetospheric boundary layer [3,5]. The low latitude portion of this boundary layer is known as the low latitude boundary layer (LLBL) and the high latitude part as the high latitude boundary layer (HLBL) which includes the plasma mantle (PM), entry layer (EL) and the polar cusp (PC) [1,3,6,7]. On the other hand, the plasma sheet boundary layer is formed due to the interaction of hot and dense plasma in the plasma sheet region with the rarified plasma of the lobe region of the magnetotail [7]. Figure 1 shows various boundary layers in the Earth's magnetosphere.



shall review the characteristics of high-frequency (wave frequency,  $f > 1$  Hz) broadband plasma waves observed in the magnetopause boundary, the polar cap boundary layer, and in the plasma sheet boundary layer. In all the above three regions, the waves could play a crucial role in the heating, acceleration and cross-field diffusion of the electrons and ions.

## 2. Magnetopause boundary layer waves

The Earth's magnetopause represents a complex variable boundary. Spacecraft observations have shown that magnetopause boundary layer is the site of ultra-low frequency (ULF) and extremely low frequency (ELF) waves. The results on both the plasma wave electric and magnetic fields in the vicinity of magnetopause were first reported by Gurnett *et al* [22] by using measurements from the ISEE 1 and 2 spacecrafts. They found that the maximum plasma wave intensities usually occur at the magnetopause. An example is shown in figure 2. They observed magnetic waves in the frequency range of 5.6 to 1 kHz characterized by a  $f^{-3.3}$  power law spectrum. The electric field turbulence occurred in the frequency range 5.6 to 100 kHz and had a featureless spectrum obeying a  $f^{-2.2}$  power law. Typical electric and magnetic field spectra of the magnetopause boundary layer waves are shown in figure 3. In a few cases, Gurnett *et al* [22] could determine that the electric field had perpendicular polarization. Gurnett *et al* [22] suggested that the magnetic waves are whistler modes, and that the electric component is a superposition of some electrostatic emissions and the electric component of the whistler mode. From the analysis of 10 ISEE 1 and 2 magnetopause crossings, Tsurutani *et al* [15] reported that both the magnetic and electric wave spectra varied by an order of magnitude in amplitude from case to case. Anderson *et al* [23] found little difference in the plasma wave characteristics at the magnetopause, in the boundary layer, and in flux transfer events (FTEs).

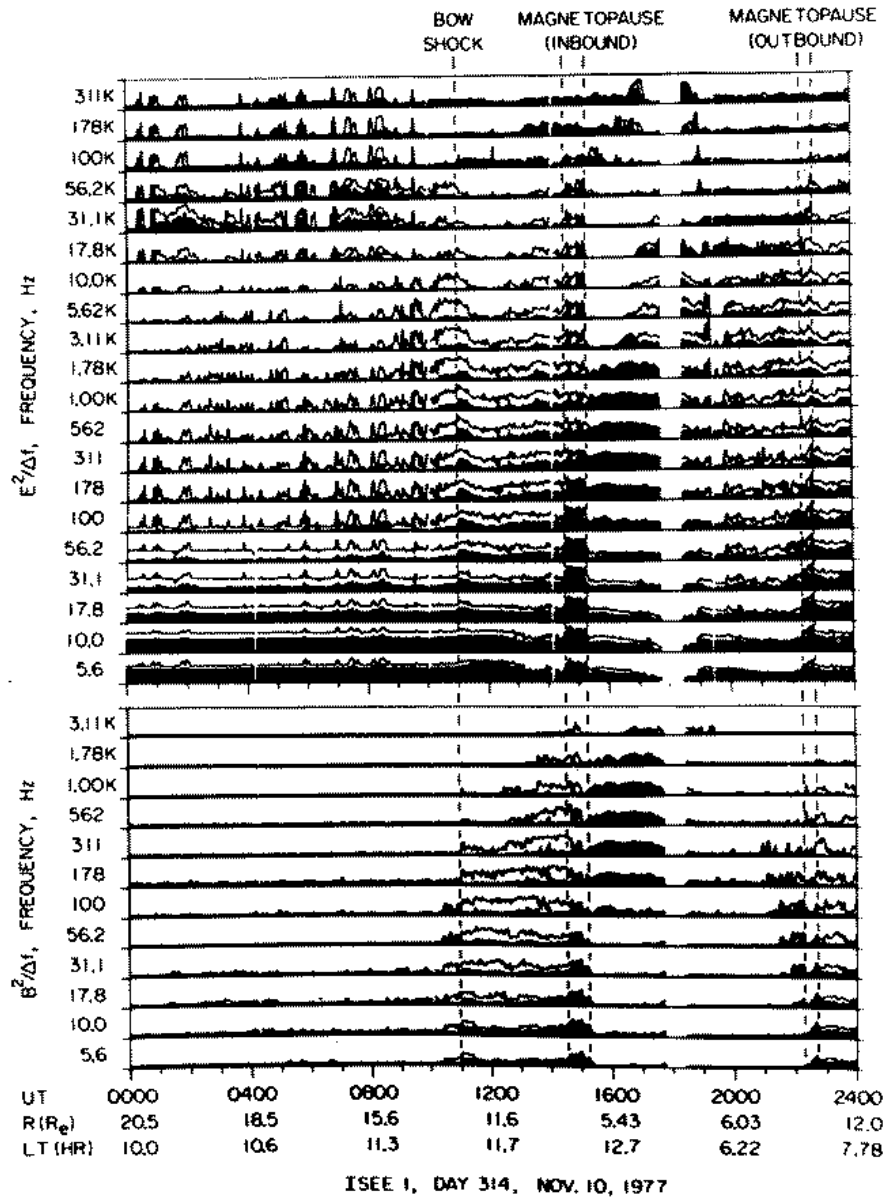
LaBelle and Treumann [24] analyzed the AMPTE/IRM plasma wave data for 3 magnetopause crossings and found that the spectrum of electric as well as magnetic fluctuations decreases with frequency as found by Gendrin [11] and Rezeau *et al* [25]. A comparison of many spacecraft observations for the magnetopause boundary layer waves as summarized by LaBelle and Treumann [24] is shown in figure 4. It is seen that nearly all of the measurements generally fit power law spectra for both electric and magnetic components.

Tsurutani *et al* [26] performed a statistical study of the broadband plasma waves at the magnetopause and showed that the correlation of the wave electric component with parameters, such as local time, latitude, magnetitude, and the  $Z$  component of IMF was quite weak. Zhu *et al* [27] found a nearly linear relationship between the local magnetic shear angle and the wave amplitudes (both electric and magnetic components). Recently, Song *et al* [28] found a clear correlation between the broadband waves and the electron plasma beta but no clear correlation between the wave amplitudes and the electron anisotropy.

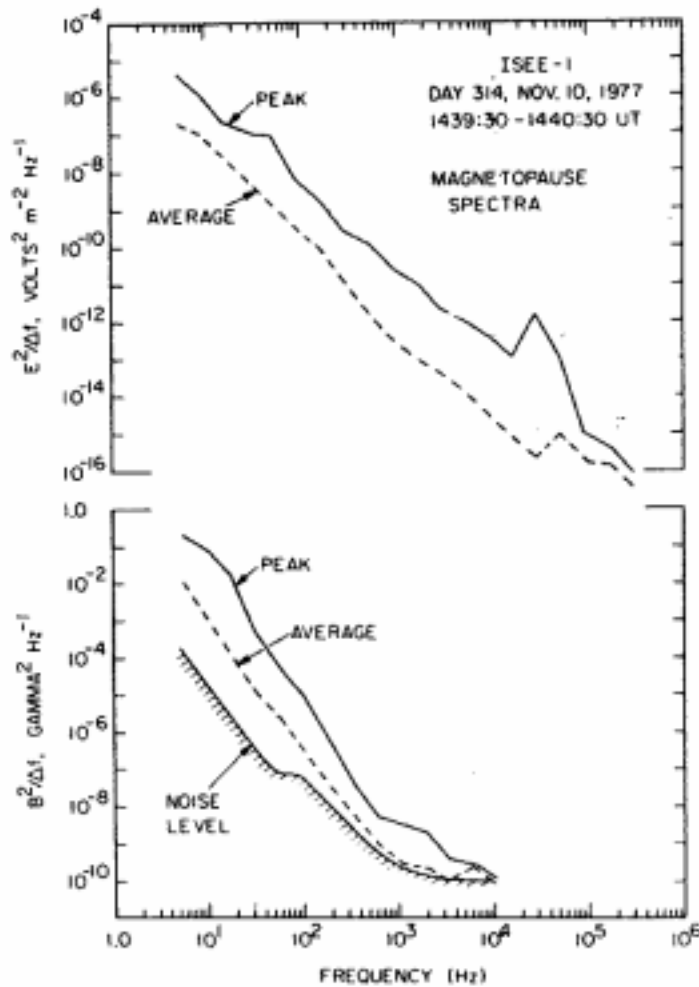
## 3. Polar cap boundary layer waves

Plasma wave data from the plasma wave instrument (PWI) [29] on the POLAR spacecraft indicate the presence of intense broadband plasma waves on the polar cap magnetic field lines which map to LLBL. These waves are spiky, and their frequency dependence and intensities are quite similar to those of the low latitude boundary layer (LLBL) waves de-

tected at and inside the low latitude dayside magnetopause (cf. §2). These waves, therefore, are called polar cap boundary layer (PCBL) waves [19].



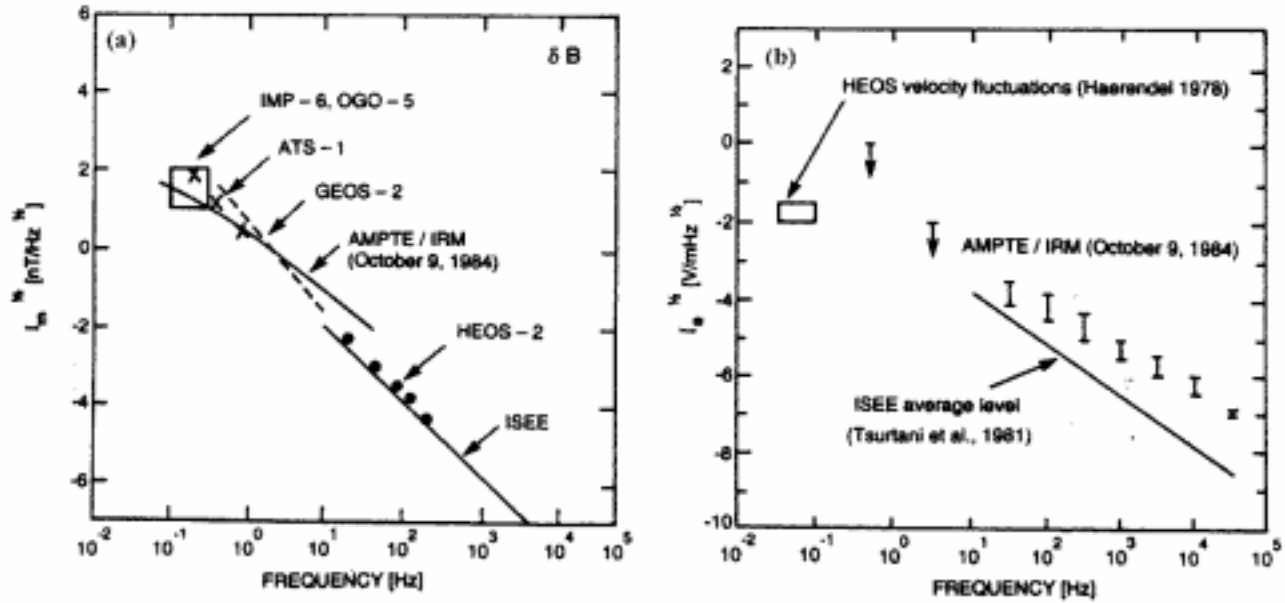
**Figure 2.** The plasma wave electric and magnetic field data from ISEE 1 for a representative pass through the magnetosphere. The enhanced electric and magnetic field intensities at the inbound and outbound magnetopause crossings are clearly indicated. From Gurnett *et al* [22].



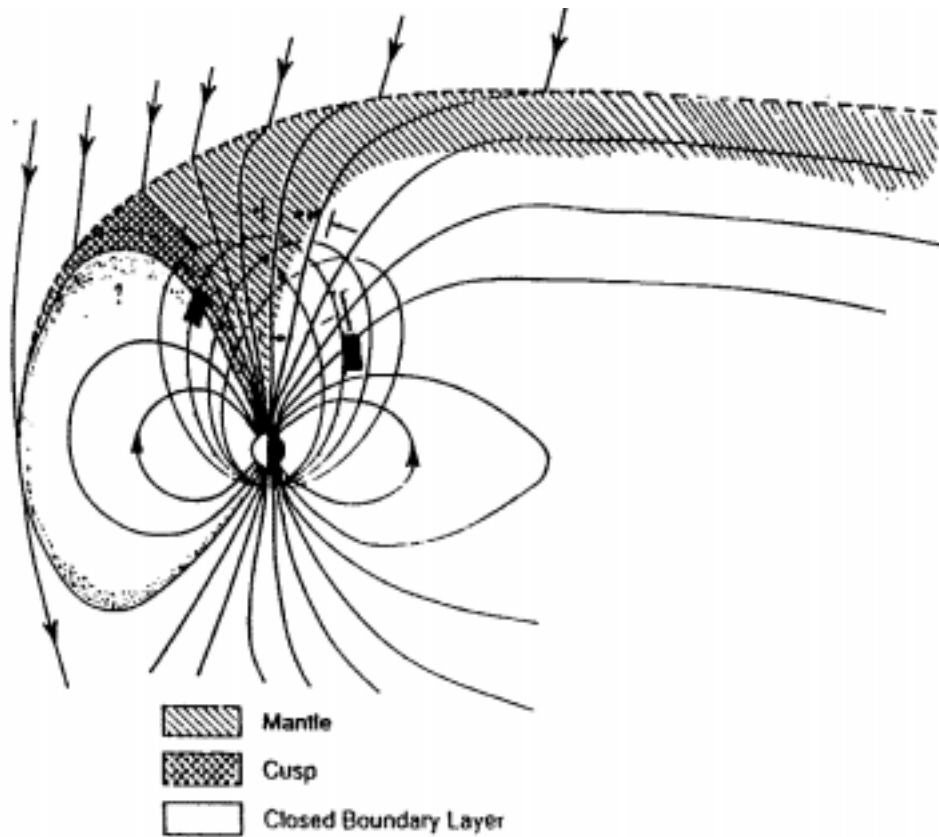
**Figure 3.** Shows the typical electric and magnetic field spectra of the enhanced plasma wave turbulence observed near the magnetopause. From Gurnett *et al* [22].

Figure 5 shows the POLAR orbit, which has an inclination of  $86^\circ$  with an apogee of  $\sim 9 R_E$  and perigee of  $\sim 1.8 R_E$  and covers the noon-midnight sector. Under ordinary circumstances the POLAR spacecraft does not intercept the magnetopause, but as shown in the figure, the spacecraft does cross field lines that map into the LLBL.

Plate 1 is a frequency-time color spectrogram of the data obtained on April 7, 1996 from the POLAR plasma wave multichannel analyzer (MCA). The electric field power spectral density is plotted according to the color bar to the right of the spectrogram. The universal time (UT), radial distance from the center of the earth ( $R_E$ ), magnetic latitude ( $\lambda_M$ ), magnetic local time (MLT), and approximate  $L$ -shell value, are indicated at the bottom of the plot. The wave intervals of interest are indicated by two sets of arrows along the



**Figure 4.** (a) The spectrum of magnetic fluctuations observed at the magnetopause from various different satellite. (b) The spectrum of electric fluctuations observed at the magnetopause from ISEE and from AMPTE/IRM. The IRM data comes from a single day; the maximum value at the magnetopause is shown, along with the spectrum averaged over the magnetopause region. The IRM data from below 30 Hz are only upper limits on the wave amplitude. Also shown is the typical value of electric field fluctuations below 0.1 Hz corresponding to the velocity fluctuations reported from the HEOS satellite. From LaBelle and Treumann [24].



**Figure 5.** The POLAR orbit and the region of wave detection (solid bar) in the magnetosphere. POLAR has a perigee at  $1.8 R_E$  and apogee at  $9 R_E$ . Waves on the field lines that map into the low latitude boundary layer (LLBL) are the topic of this study. From Tsurutani *et al* [19].

time axis, and are designated as ‘dayside PCBL’ and ‘nightside PCBL’ within plate 1. These intervals of intense waves bound magnetic fields that map into the polar cap region. Both wave events occur in the northern hemisphere near apogee. The dayside PCBL event occurs near 13.0 MLT and the other near 0.3 MLT, as the spacecraft orbit is in a near noon-midnight orientation. The PCBL waves are characterized by bursts of ‘turbulence’ covering a broad frequency range extending from  $f < 10^1$  to  $2 \times 10^4$  Hz as shown in the MCA electric field spectrum of plate 1. The magnetic field spectrum for these waves shows similar bursts (not shown). The region between the dayside PCBL and the nightside PCBL (about 0555 to 1450 UT) is identified as the northern polar cap. In this region there is typically a lack of strong signals although a few bursts of electrostatic noise are seen, as well as auroral hiss (3 kHz) and auroral kilometric radiation (100 kHz).

Analysis of the PWI data from March 13 to August 31, 1996 on the dayside (05 to 18 GMT) near POLAR apogee in the northern hemisphere, consisting of 254 ‘crossing’

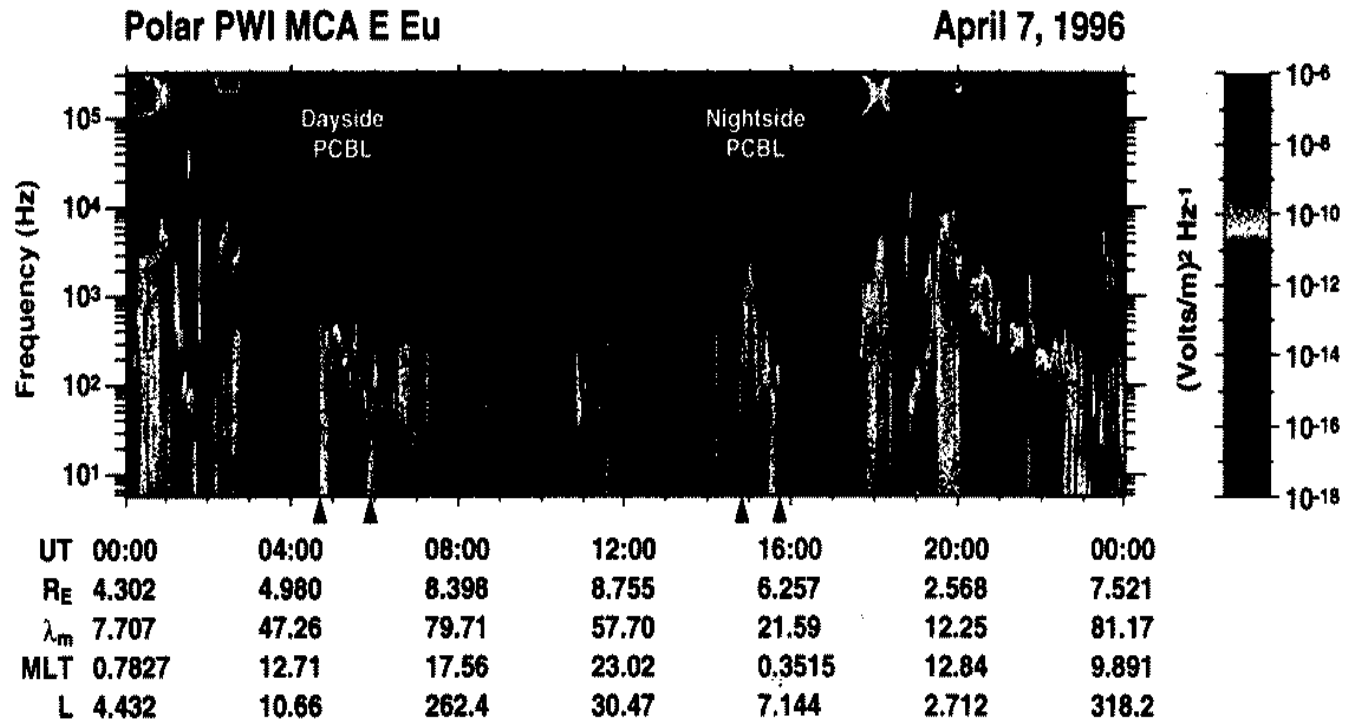


**Plate 1.** Color spectrogram of wave electric field from  $\sim 10^1$  to  $10^4$  Hz and above. The boundary layer waves are indicated. In between the two boundary layer (dayside and nightside) crossings is the polar cap (quiet wave region). From Tsurutani *et al* ([19], plate 1).

of the PCBL field lines, shows that the waves are present nearly all the time. The region of PCBL wave activity is located in a relatively narrow band of latitudes from  $70^\circ$  to  $85^\circ$ . The wave location is slightly lower than cusp field lines. There is a trend for the PCBL waves to extend to slightly lower latitudes in both the dawn and dusk sides relative to the noon sector. Furthermore, the PCBL waves occur predominantly in the region with  $L \sim 10$  or larger. Further, the intense noon sector wave events are found to be well correlated with enhanced fluxes of 10 to 200 eV  $H^+$ ,  $He^{++}$  and  $O^+$  ions.

The spectral density plots for both electric and magnetic field are found to have rough power-law shapes, even though the intensities and spectral shapes vary from event-to-event. The electric component has on average a  $f^{-2.2}$  frequency dependence, and the wave frequency extends from  $\sim 10^1$  Hz to  $\sim 2 \times 10^4$  Hz, whereas the wave magnetic component has on average a  $f^{-2.7}$  frequency dependence and appears to have an upper frequency cut-off at the electron cyclotron frequency. The electric and magnetic spectra of a typical event occurring near the apogee in the northern hemisphere on day 98, 1996 at 1302 MLT at  $78.8^\circ$  N invariant magnetic latitude is shown in figures 6. Note that the electric component of the waves extends to frequencies above the electron cyclotron frequency. Although it appears that the wave magnetic component cuts off at the electron cyclotron frequency,  $f_{ce}$ , this is too close to the noise floor of the receiver to make any definite determination.

The PCBL waves occur on field lines that map into or close to the LLBL field lines, and the wave characteristics are quite similar to those of the LLBL waves. An inter-comparison between the POLAR wave power spectra and the LLBL waves as measured by ISEE-1 and -2 and GEOS is given in table 1. The GEOS event, which is much more intense than either ISEE-1 and -2 or POLAR wave intensities, is somewhat anomalous as it occurred during a magnetic storm when the magnetopause was pushed into the spacecraft orbit ( $6.6 R_E$ ). It is possible that the extraordinarily high solar wind ram pressure and intense southward interplanetary magnetic field  $B_s$  may have led to unusually high wave power during this event. Table 1 also lists a spectrum for day 103, 1996 for POLAR when it was near the southern hemisphere dayside perigee at  $\sim 2 R_E$ . We note that the wave intensities are of the same order as the high altitude northern hemispherical events.

A schematic of the magnetic field lines, the PCBL wave locations and the LLBL wave locations is shown in figure 7. Although to date such waves have been identified at only three regions along the field lines (PCBL, LLBL and POLAR near-perigee), one can argue that the waves most likely exist along the entire length of the field lines provided that the field lines are 'closed' and extend from one hemispherical ionosphere to the other. The PCBL wave field lines must be configured as indicated in figure 7, where they map into the earth's ionosphere over a broad region of local times. The three-point intensity (LLBL, POLAR near-apogee, POLAR near-perigee) measurements put strong constraints on the wave source location. The most likely scenario appears to be the wave generation by a local source of free energy existing along field lines. Two possible sources are field-aligned currents and density gradients [30–33].

#### 4. Plasma sheet boundary layer waves

Broadband electrostatic emissions were observed around the plasma sheet boundary layer by Gurnett *et al* [17]. They referred to these emissions as 'broadband electrostatic noise (BEN).' Gurnett *et al* [17] reported BEN's detailed features using the plasma wave data

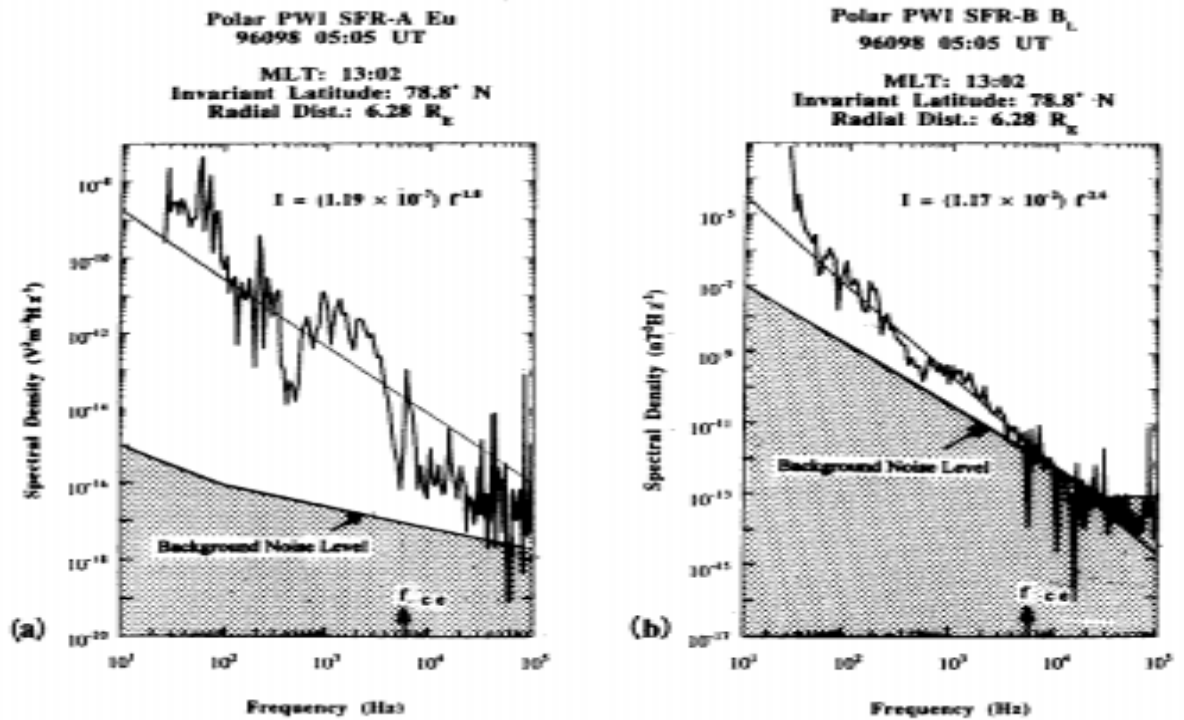


**Figure 6.** The electric field (a) and magnetic field (b) spectra for the events occurring on day 098, 1996. The background noise is indicated. The electric component of the waves extend beyond the electron cyclotron frequency ( $\sim 6 \times 10^3$  Hz). From Tsurutani *et al* [19].

**Table 1.** Comparison of broadband plasma wave properties in various boundary layers.

Spacecraft	Location	Date	$\frac{B}{(nT)^2} \text{ Hz}^{-1}$	$\frac{E}{V^2 \text{ m}^{-2} \text{ Hz}^{-1}}$
POLAR <sup>1</sup>	$\sim 7-8 R_E$ altitude	day 098, 1996	$1.17 \times 10^{-2} f^{-2.6}$	$1.19 \times 10^{-7} f^{-1.8}$
	$\sim 2 R_E$ altitude	day 103, 1996	$1.34 \times 10^{-2.5} f^{-2.5}$	$1.22 \times 10^{-6} f^{-1.8}$
ISEE <sup>2</sup> 1	Earth's LLBL	day 314, 1977	$\sim f^{-3.3}$	$\sim f^{-2.2}$
ISEE <sup>3</sup> 1, 2	Earth's LLBL	1977	$1.0 \times 10^1 f^{-3.9}$	$3.0 \times 10^{-5} f^{-2.8}$
ISEE <sup>4</sup> 1, 2	Earth's LLBL	1977	$7.90 \times 10^{-2} f^{-2.9}$	$6.3 \times 10^{-6} f^{-2.2}$
GEOS <sup>5</sup> 2	Earth's LLBL	day 240, 1978	$3.60 \times 10^1 f^{-2.6}$	$1.2 \times 10^{-6} f^{-2.6}$
ISEE <sup>6</sup> 1	Earth's LLBL	1977-1978	$3.0 \times 10^{-1} f^{-3.3}$	$6.0 \times 10^{-7} f^{-2.1}$

<sup>1</sup>Tsurutani *et al* [19]; <sup>2</sup>Gurnett *et al* [22]; <sup>3</sup>Tsurutani *et al* [15]; <sup>4</sup>Anderson *et al* [23]; <sup>5</sup>Rezeau *et al* [25]; <sup>6</sup>Tsurutani *et al* [26].

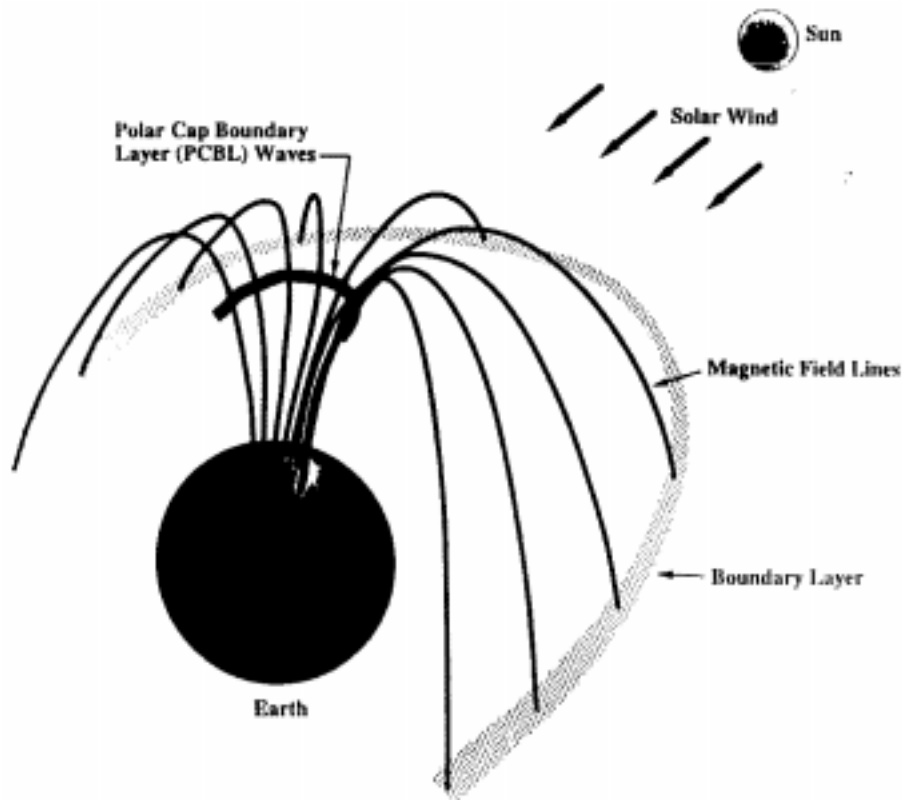


**Figure 7.** A northern polar view of the mapping of polar cap boundary layer (PCBL) waves to the low latitude boundary layer (LLBL). From Tsurutani *et al* [19].

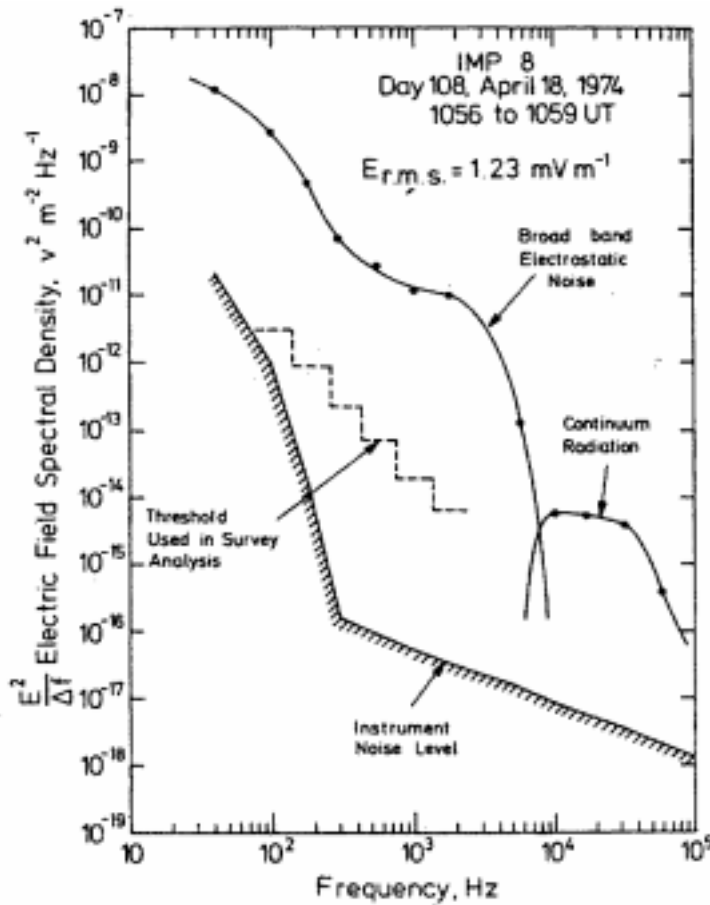


**Figure 8.** A typical frequency spectrum of the broadband electrostatic noise observed by the IMP 8 spacecraft (figure 5 in Gurnett *et al* [17]).

observed by IMP-8, which passes through the magnetotail at radial distances ranging from about  $23 R_E$  to  $46 R_E$ . Figure 8 shows a typical spectrum of BEN reported by Gurnett *et al* [17]. BEN usually occurs over a broad range of frequencies extending from about 10 Hz to a few kHz with intensities ranging from about  $50 \mu\text{V}/\text{m}$  to  $5 \text{ mV}/\text{m}$ . BEN consists of many discrete bursts lasting from a few seconds to several minutes. The spectrum shows a marked decrease in intensity at the electron cyclotron frequency and a lower cutoff at the local lower hybrid resonance frequency. The wave electric field was found to be oriented within  $\pm 20^\circ$  from perpendicular to the magnetic field. BEN is commonly observed in the plasma sheet boundary layer with a strong correlation with high energy ion flows.

On the other hand, Parks *et al* [34] demonstrated the relation of the BEN and electron beams based on the observations by ISEE-1 spacecraft. Onsager *et al* [35] showed that BEN can be observed in the electron layer of the outer PSBL without energetic ions. They pointed out that the ion streaming is not essential for the excitation of BEN, and stressed that BEN has a close relationship to the electron dynamics.

## 5. Generation mechanisms

The plasma waves observed in the magnetopause BL, the PSBL, or in the PCBL are broadband with no obvious spectral peaks which could be used to identify the plasma instabilities exciting these modes. As the boundary layers are the sites of many free energy sources existing simultaneously, it is not an easy task to identify which free energy source could be dominant for a given event. The changing interplanetary conditions can further complicate the identification of the free energy source and relevant plasma instability driven by it. The gradients in density, temperature, velocity and magnetic field, sometimes all together, are present at the boundary layers. These gradients could act as sources of free energy for wave generation. In addition, the boundary layers can support strong currents, particle beams, and anisotropic velocity space distributions, which again can drive many plasma instabilities [21].

A number of possible wave modes have been put forth in the literature for the BL waves. Some of the important generation models are based on the lower hybrid drift instability (LHDI) driven essentially by the density gradients [36–38], field-aligned current driven instabilities, like ion-acoustic instability [39], and ion cyclotron instability [40], ion beam instabilities [41–47], electron beam instabilities [34,35,48–51], loss cone instabilities generated by the electron loss distributions [52], and velocity shear and current convective instabilities [27,29,30,53–57]. The mechanism of current convective instability demands thickness of the magnetopause current layer,  $L$ , to be very narrow such that  $L < \delta_e$ , where  $\delta_e = c/\omega_{pe}$  ( $c$  and  $\omega_{pe}$  are the speed of light and the electron plasma frequency, respectively) is the electron skin depth. The whistler instability on the other hand requires that  $L < \delta_i$ , where  $\delta_i = c/\omega_{pi}$  is the ion skin depth. The observed thickness of the magnetopause is typically several times the ion skin depth. Although all these mechanisms can explain the strongest wave power at the lowest frequencies, they suffer from a common drawback as to how to cascade the power up to VLF frequencies.

Lakhina and Tsurutani [33] have presented a linear theory for the generation of broadband PCBL plasma waves. Their coupled velocity shear-lower hybrid instabilities model based on two-fluid equations, is fully electromagnetic and takes into account the free energy available due to the presence of field-aligned currents, and gradients in the currents, the plasma densities and the magnetic fields. The dispersion relation generalizes the dispersion relations for several plasma modes, including the lower hybrid [36], the modified-two stream instability [58], beam modes [44,59] current convective and whistler instabilities [30,31]. In general, the beam driven modes, the current convective and the lower hybrid drift modes are coupled, and the dispersion relation has to be solved numerically. It is found that density gradients tend to stabilize both the current convective and the whistler instabilities, at the same time these modes develop real frequencies. On the other hand, sharp density gradients can lead to the excitation of a lower hybrid drift instability when the hot ions are present in the boundary layer.

## 6. Resonant wave particle interactions

All the three boundary layers, namely, the magnetopause BL, the polar cap BL and the plasma sheet BL, constitute more or less a collisionless plasma system. However, the interaction of broadband plasma waves with the charged particles can cause scattering of the

particles thereby changing particles' momenta and energies. Thus wave-particle interactions in a collisionless plasma can play a role similar to direct particle-particle collisions in a collisional plasma. A particle can interact strongly with the waves when it senses the wave Doppler-shifted to its cyclotron frequency (or its harmonics). This process is known as cyclotron resonance. The condition for the cyclotron resonance between the waves and the particles can be written as

$$\omega - k_{\parallel} v_{\parallel} = n\Omega, \tag{1}$$

where  $\omega$  and  $k_{\parallel}$  are the wave frequency and the parallel component of the wave vector  $\mathbf{k}$ ,  $v_{\parallel}$  is the parallel component of the particle velocity,  $\Omega = qB_0/mc$  is the cyclotron frequency of the charged particle,  $B_0$  is the magnetic field,  $q$  and  $m$  are particle charge and mass, respectively,  $c$  is the speed of light, and  $n$  is an integer equal  $0, \pm 1, \pm 2, \dots$ . The  $k_{\parallel} v_{\parallel}$  term is the Doppler shift effect due to the particle motion relative to the wave. The case of  $n = 0$  corresponds to the Landau resonance. When condition (1) is satisfied, the waves and particles remain in phase, leading to energy and momentum exchange between them.

Tsurutani and Thorne [8] have given general expressions for cross-field diffusion of electrons and ions via resonant interaction with either electromagnetic or electrostatic waves. The cross-field diffusion rate due to the magnetic component of electromagnetic waves can be written as [8,12,13]

$$D_{\perp,B} = 2\eta \left( \frac{B}{B_0} \right)^2 D_{\max}, \tag{2}$$

where  $B$  is the amplitude of the wave magnetic field at the resonant frequency given by eq. (1),  $\eta$  is a dimensionless scaling factor indicating what fraction of time the particles stay in resonance with the waves, and

$$D_{\max} = \frac{cmv_{\perp}^2}{2\epsilon B_0} \tag{3}$$

is the Bohm diffusion rate [60]. Here,  $v_{\perp}$  denotes perpendicular velocity of the charged particles relative to the ambient magnetic field  $\mathbf{B}_0$ .

The cross-field diffusion rate due to the electrostatic waves is given by

$$D_{\perp,E} = 2\eta \left( \frac{E}{B_0} \right)^2 \left( \frac{c}{v} \right)^2 D_{\max}, \tag{4}$$

where  $E$  is the amplitude of the wave electric field at the resonant frequency given by eq. (1), and  $v$  is the magnitude of the particle velocity.

For the boundary layer parameters,  $B_0 \approx 50$  nT,  $N \approx 20$  cm<sup>-3</sup>, protons of energies  $\sim 1$  keV can be in cyclotron resonance with the wave at  $\omega/\Omega_p \sim 1$  ( $\Omega_p$  is the proton cyclotron frequency), i.e., at frequencies close to 1 Hz. Using the observed power at these frequencies in wave magnetic [11,25] and electric [15] components, we get  $D_{\perp,B} = 260$  km<sup>2</sup> s<sup>-1</sup> and  $D_{\perp,E} \approx 4 \times 10^2$  km<sup>2</sup> s<sup>-1</sup> for  $\sim 1$  keV protons, with negligible cross-field diffusion for 1 keV electrons.

It should be noted that theoretical models of either a viscous momentum transfer or mass diffusion across the magnetopause [61] require a kinematic viscosity or diffusion

coefficient comparable to  $10^3 \text{ km}^2 \text{ s}^{-1}$  to account for the observed magnetopause boundary layer thickness. Since the broadband waves show significant variability in the power spectral densities for both magnetic and electric components [11,15,22,24,25], this could lead to substantially different rates of cross-field diffusion thereby explaining the observed variations in the thickness of the magnetopause boundary layer.

The intense broadband waves in the boundary layers can cause rapid isotropization of both the electron and the ion distributions. Tsurutani *et al* [15] found a strong correlation between intense broadband waves in the magnetopause BL and 1–6 keV electrons and protons. The observed wave power was found to be sufficient to scatter the 1–6 keV electrons and protons near the limit of strong pitch angle diffusion. On using the measured spectrum of the ISEE-1 electrons and ions and integrating from 1 to 10 keV, the precipitated energy flux into the atmosphere was estimated to be  $\approx 1.0 \text{ erg cm}^{-2} \text{ s}^{-1}$  [26]. These numbers are comparable to the dayside auroral energy input. The presence of PCBL waves would further increase the above estimate. Therefore, it appears that resonant cyclotron interactions between the waves and particles in the magnetopause and polar cap boundary layers can provide a reasonable explanation for the nearly continuous presence of dayside aurora.

## 7. Fine structure of boundary layer waves

Most of the above observation results and data analyses of the broadband boundary layer waves were discussed in the frequency domain. Only recently high time resolution boundary layer wave data have been analysed. The waveform observations by the plasma wave instrument on board the Geotail spacecraft have shown that BEN consists of a series of bipolar solitary pulses [50]. The widths of the BEN frequency spectra arise from the solitary waveforms. A likely generation mechanism for BEN is based on the nonlinear evolution of electron beam instabilities leading to the formation of the isolated Bernstein-Greene-Kruskal (BGK) [62], potential structures which reproduce well the observed electrostatic solitary waveforms [51,63].

The high time resolution measurements of the broadband plasma waves in the PCBL region by Polar and in the auroral ionosphere by FAST (fast auroral snapshot) have just started to come out, and they have given very useful information on the fine structure of the BL waves. Recent results on the PCBL waves using the high time resolution of the POLAR, shown in figure 9 indicate the presence of large amplitude bipolar pulses (bpp) in the parallel electric component of the wave, similar to PSBL BEN, at high altitudes ( $\sim 6 R_E$ ) [64,65] as well as low altitudes ( $\sim 1-2 R_E$ ) [66]. There are magnetic signatures associated with these electric pulses. Offset bipolar pulses (obpp), where the positive pulse does not follow immediately after the negative pulse, but are delayed somewhat, are also seen in this figure. Further, the monopolar pulses (mpp) in the parallel electric field component are seen in the right-hand inset of figure 9. The monopolar pulses are found to alternate between one polarity and the opposite polarity, and to occur in pairs.

Similarly, recent measurements from FAST have revealed the presence of intense localized electrostatic wave structures at altitudes of 2000 to 4000 km on the auroral field lines. Muschietti *et al* [67] have interpreted these solitary structures [68,69] in terms of BGK phase-space electron holes drifting along the magnetic field lines. Goldman *et al* [70] have given an explanation for these bipolar structures in terms of nonlinear two-stream instabilities, a mechanism similar to that of PSBL BEN proposed by Omura *et al* [51] and Kojima *et al* [63].

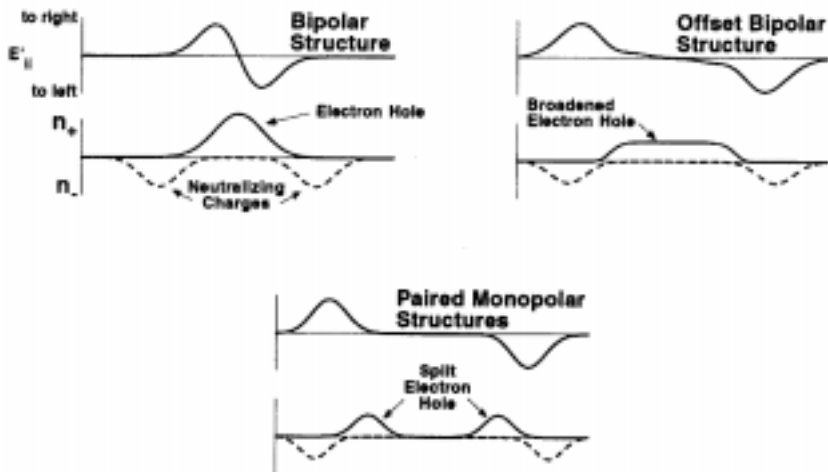


**Figure 9.** Bipolar (bpb), offset bipolar (obpb), and monopolar (mpb) wave structures in parallel electric field component. From Tsurutani *et al* [65].

## 8. Conclusion

Interaction of solar wind with the magnetosphere provides a dynamic Sun–Earth plasma connection. The magnetopause, the polar cap, and the plasma sheet boundary layers, which are formed due to solar wind magnetosphere interaction, are the sites of broadband plasma waves. We have described the main characteristics of the broadband plasma waves observed in the Earth’s magnetopause BL, PCBL, and in the plasma sheet BL. The waves are spiky signals spanning a broad frequency range from less than the ion cyclotron frequency to probably greater than electron cyclotron frequency. The magnetopause and polar cap BL waves could scatter the energetic electrons and ions into the atmospheric loss cone. The energy flux precipitated into the auroral ionosphere is sufficient to excite dayside aurora. Since the magnetopause and the polar cap boundary field lines map to the auroral oval, it is suggested that these boundary layer waves are responsible for the diffused dayside aurora.

It appears that the broadband plasma waves discussed here are ubiquitous to the plasma flow boundary layers. For example, BEN has been observed in the magnetotail [50,63,71,72], on cusp and auroral field lines [68,72–75], and in the magnetosheath [23]. The magnetotail BEN emissions are correlated with ion and electron beams, whereas auroral region BEN emissions are usually associated with ion conics and field-aligned electron beams. Dubouloz *et al* [75] have proposed a generation mechanism for auroral field line BEN in terms of electron acoustic solitons.

The waveform observations by the plasma wave instrument on board the Geotail, Polar and FAST spacecraft have shown that BEN consists of a series of bipolar solitary pulses. The solitary structures appear to be phase space holes due to the formation of Greene-Kruskal (BGK) potential structures.

We would like to point out that the mechanism discussed by Dubouloz *et al* [75] predict negatively charged structures whereas the Geotail [51], the POLAR [64] as well as FAST [68,69] observations indicate positively charged flowing potential structures. It is important to note that a potential structure, whether positive or negative, must inherently be a part of

some nonlinear wave where the charges are trapped, otherwise it would rapidly disrupt due to the repulsive forces of the charges. Depending on the free energy available, some of the instabilities discussed in §5 could evolve nonlinearly into solitary waves, for example, whistler-type solitons. If this happens it would naturally explain the recent observations on the waveform of the coherent structures (including the associated magnetic component, if any).

Further analyses of the high time resolution plasma and wave data from Polar, FAST and Geotail would lead to a better understanding of the BL waves and their role in cross-field particle diffusion leading to the formation of the boundary itself, and in the processes of heating/acceleration and precipitation of the BL plasma causing the dayside aurora.

## **Acknowledgments**

A part of this research effort was performed at the Jet Propulsion Laboratory, California Institute of Technology, Pasadena, under contract with the National Aeronautics and Space Administration. The research at Indian Institute of Geomagnetism, Mumbai was supported by the Department of Science and Technology, Government of India.

## **References**

- [1] E W Hones Jr, J R Asbridge, S J Bame, M D Montgomery, S Singer and S-I Akasofu, *J. Geophys. Res.* **77**, 5503 (1972)
- [2] S-I Akasofu, E W Hones Jr, S J Bame, J R Asbridge and A T Y Lui, *J. Geophys. Res.* **78**, 7257 (1973)
- [3] T E Eastman, E W Hones Jr, S J Bame and J R Asbridge, *Geophys. Res. Lett.* **3**, 685 (1976)
- [4] G Haerendel, G Paschmann, N Sckopke, H Rosenbauer, and P C Hedgecock, *J. Geophys. Res.* **83**, 3195 (1978)
- [5] R Lundin, *Phys. Scr.* **18**, 85 (1987)
- [6] H Rosenbauer, H Grunwaldt, M D Montgomery, G Paschmann and N Sckopke, *J. Geophys. Res.* **80**, 2723 (1975)
- [7] G Haerendel and G Paschmann, *Magnetospheric Plasma Physics* edited by A Nishida (Center for Academic Publications, Japan, Tokyo, 1982)
- [8] B T Tsurutani and R M Thorne, *Geophys. Res. Lett.* **22**, 663 (1982)
- [9] W Baumjohann and G Paschmann, *Phys. Scr.* **T18**, 61 (1987)
- [10] L C Lee, J R Johnson and Z W Ma, *J. Geophys. Res.* **99**, 17405 (1994)
- [11] R Gendrin, *Geophys. Res. Lett.* **10**, 769 (1983)
- [12] R M Thorne and B T Tsurutani, *Physics of Space Plasmas (1990)* edited by T Chang *et al* (Sci. Publ. Inc., Cambridge, MA, 1991) vol. 10, p. 119
- [13] B T Tsurutani and G S Lakhina, *Rev. Geophys.* **35**, 491 (1997)
- [14] W I Axford and C O Hines, *Can. J. Phys.* **39**, 1433 (1961)
- [15] B T Tsurutani, E J Smith, R M Thorne, R R Anderson, D A Gurnett, G K Parks, C S Lin and C T Russell, *Geophys. Res. Lett.* **8**, 183 (1981)
- [16] F L Scarf, L A Frank, K L Ackerson and R P Lepping, *Geophys. Res. Lett.* **1**, 189 (1974)
- [17] D A Gurnett, L A Frank and R P Lepping, *J. Geophys. Res.* **81**, 6059 (1976)
- [18] T E Eastman, L A Frank, W K Peterson, and W Lennartsson, *J. Geophys. Res.* **89**, 1553 (1984)
- [19] B T Tsurutani, G S Lakhina, C M Ho, J K Arballo, C Galvan, A Boonsiriseth, J S Pickett, D A Gurnett, W K Peterson and R M Thorne, *J. Geophys. Res.* **103**, 17351 (1998)

- [20] G S Lakhina and B T Tsurutani, *Surveys Geophys.* (in press) (1999)
- [21] G S Lakhina, B T Tsurutani, H. Kojima and H Matsumoto, *J. Geophys. Res.* (in press) (2000)
- [22] D A Gurnett, R R Anderson, B T Tsurutani, E J Smith, G Paschmann, G Haerendel, S J Bame and C T Russell, *J. Geophys. Res.* **84**, 7043 (1979)
- [23] R R Anderson, C C Harvey, M M Hoppe, B T Tsurutani, T E Eastman, and J Etcheto, *J. Geophys. Res.* **87**, 2087 (1982)
- [24] J LaBelle, and R A Treumann, *Space Sci. Rev.* **47**, 175 (1988)
- [25] L Rezeau, S Perraut and A Roux, *Geophys. Res. Lett.* **13**, 1093 (1986)
- [26] B T Tsurutani, A L Brinca, E J Smith, R T Okida, R R Anderson and T E Eastman, *J. Geophys. Res.* **94**, 1270 (1989)
- [27] Z Zhu, P Song, J F Drake, C T Russell, R R Anderson, D A Gurnett, K W Ogilvie and R J Fitzenreiter, *Geophys. Res. Lett.* **23**, 773 (1996)
- [28] P Song, J Zhu, C T Russell, R R Anderson, D A Gurnett, K W Ogilvie, R J Strangeway, *J. Geophys. Res.* **103**, 26495 (1998)
- [29] D A Gurnett, *Space Sci. Rev.* **71**, 597 (1995)
- [30] J F Drake, J Gerber and R G Kleva, *J. Geophys. Res.* **99**, 11211 (1994a)
- [31] J F Drake, R G Kleva and M E Mandt, *Phys. Rev. Lett.* **73**, 1251 (1994b)
- [32] G S Lakhina, B T Tsurutani, J K Arballo, C M Ho and A Boonsiriseth, *EOS* **78**, S297 (1997)
- [33] G S Lakhina, and B T Tsurutani, *J. Geophys. Res.* **104**, 279 (1999)
- [34] G K Parks, M McCarthy, R J Fitzenreiter, J Etcheto, K A Anderson, R R Anderson, T E Eastman, L A Frank, D A Gurnett, C Huang, R P Lin, A T Y Lui, K W Ogilvie, A Pedersen, H Reme and D J Williams, *J. Geophys. Res.* **89**, 8885 (1984)
- [35] T G Onsager, M F Thomsen, R C Elphic, J T Gosling, R R Anderson and G Kettmann, *J. Geophys. Res.* **98**, 15509 (1993)
- [36] S P Gary and T E Eastman, *J. Geophys. Res.* **84**, 7378 (1979)
- [37] J D Huba, N T Gladd and J F Drake, *J. Geophys. Res.* **86**, 5881 (1981)
- [38] P Revathy and G S Lakhina, *J. Plasma Phys.* **17**, 133 (1977)
- [39] Kindel and C F Kennel, *J. Geophys. Res.* **76**, 3055 (1971)
- [40] M Ashour-Abdalla and R M. Thorne, *J. Geophys. Res.* **83**, 4775 (1978)
- [41] S P Gary, C W Smith, M A Lee, M L Goldstein and D W Forslund, *Phys. Fluids* **27**, 1852 (1984) (Erratum, *Phys. Fluids* **28**, 438 (1985))
- [42] F Verheest and G S Lakhina, *J. Geophys. Res.* **96**, 7905 (1991)
- [43] F Verheest and G S Lakhina, *J. Geophys. Res.* **98**, 21017 (1993)
- [44] G S Lakhina, *Annales Geophysicae* **64**, 660 (1993)
- [45] C L. Grabbe and T E Eastman, *J. Geophys. Res.* **89**, 3865 (1984)
- [46] K Akimoto and N Omid, *Geophys. Res. Lett.* **13**, 97 (1986)
- [47] M Ashour-Abdalla and H Okuda, *J. Geophys. Res.* **91**, 6833 (1986)
- [48] D Schriver and M Ashour-Abdalla, *Geophys. Res. Letts.* **16**, 899 (1989)
- [49] W Baumjohann, R A Treumann, J LaBelle and R R Anderson, *J. Geophys. Res.* **94**, 15221 (1989)
- [50] H Matsumoto, H Kojima, T Miyatake, Y Omura, M Okada and M Tsutsui, *Geophys. Res. Lett.* **21**, 2915 (1994)
- [51] Y Omura, H Matsumoto, T Miyake and H Kojima, *J. Geophys. Res.* **101**, 2685 (1996)
- [52] C F Kennel and H E Petschek, *J. Geophys. Res.* **71**, 1 (1966)
- [53] N D' Angelo, *Rev. Geophys.* **15**, 299 (1973)
- [54] A Miura, *J. Geophys. Res.* **92**, 3195 (1987)
- [55] G S Lakhina, *J. Geophys. Res.* **92**, 12161 (1987)
- [56] G S Lakhina, *Phys. Scr.* **T50**, 114 (1994)
- [57] G Ganguli, M J Keskinen, H Romero, R Heelis, T Moore and C Pollock, *J. Geophys. Res.* **99**, 8873 (1994)

- [58] G S Lakhina and A Sen, *Nucl. Fusion* **13**, 913 (1973)
- [59] C T Dum, *J. Geophys. Res.* **94**, 2429 (1989)
- [60] D Bohm, *Characteristics of electrical discharges in magnetic fields* edited by A Guthrie and R Walkerling (McGraw Hill, New York, 1949) p. 1
- [61] B U Sonnerup, *J. Geophys. Res.* **85**, 2017 (1980)
- [62] I B Bernstein, J M Greene and M D Kruskal, *Phys. Rev.* **108**, 546 (1957)
- [63] H Kojima, H Matsumoto, S Chikuba, S Horiyama, M Ashour-Abdalla and R R Anderson, *J. Geophys. Res.* **102**, 14439 (1997)
- [64] J R Franz, P M Kintner, J S Pickett, *Geophys. Res. Lett.* **25**, 1277 (1998)
- [65] B T Tsurutani, J K Arballo, G S Lakhina, C M Ho, B Buti, J S Pickett and D A Gurnett, *Geophys. Res. Lett.* **25**, 4117 (1998b)
- [66] F S Mozer, R Ergun, M Temerin, C Cattell, J Dombeck and J Wygant, *Phys. Rev. Lett.* **79**, 1281 (1997)
- [67] L Muschietti, R E Ergun, I Roth and C W Carlson, *Geophys. Res. Lett.* **26**, 1093 (1999)
- [68] R E Ergun *et al.*, *Geophys. Res. Lett.* **25**, 2041 (1998)
- [69] R E Ergun, C W Carlson, J P Fadden, F S Mozer, L Muschietti, I Roth and R Strangeway, *Phys. Rev. Lett.* **81**, 826 (1998)
- [70] M V Goldman, M M Oppenheim and D L Newman, *Geophys. Res. Lett.* **26**, 1821 (1999)
- [71] C A Cattell, F S Mozer, R R Anderson, E W Hones Jr and R D Sharp, *J. Geophys. Res.* **91**, 5681 (1986)
- [72] D A Gurnett and L A Frank, *J. Geophys. Res.* **82**, 1031 (1977)
- [73] D A Gurnett and L A Frank, *J. Geophys. Res.* **82**, 1447 (1978)
- [74] R Pottelette, M Malingre, N Dubouloz, B Aparicio, R Lundin, G Holmgren and G Marklund, *J. Geophys. Res.* **95**, 5957 (1990)
- [75] N Dubouloz, R Pottelette, M Malingre, G Holmgren and P A Lindqvist, *J. Geophys. Res.* **96**, 3565 (1991)